

Cross Polarization Conversion and RCS Reduction Using Venus-Like Metallic Resonators

Mustafa K. Taher Al-Nuaimi^{1,2} and Yejun He¹

¹*Guangdong Engineering Research Center of Base Station Antennas and Propagation, Shenzhen Key Laboratory of Antennas and Propagation, College of Information Engineering, Shenzhen University, 518060, China*

²*State Key Laboratory of Millimeter Waves, Southeast University, Nanjing, 210009, China
Email: mustafa.engineer@yahoo.com, heyejun@126.com*

Abstract—This paper presents the design of low backscattered non-absorptive reflective surface at W-band. The presented non-absorptive reflective surface is designed based on cross-polarization conversion principle in which a simple geometry copper unit cell of Venus-like shape is used to compose the surface. The unit cell has three plasmon resonance frequencies at about 96GHz, 97.4GHz, and 99GHz. The unit cell can convert the incident x- or y-polarized EM-waves to their orthogonal components with more than 90% cross-polarization conversion efficiency from about 95.7GHz to 99.3GHz. Moreover, if the proposed unit cell along with its mirrored unit cell are precisely designed and randomly distributed across the surface aperture and arranged in 2D lattice, then $180^\circ \pm 30^\circ$ of reflection phase difference (cancellation) is valid and a low-level backscattered diffuse radar cross section patterns can be obtained.

Index Terms—polarization conversion, cross-polarization, millimeter wave, radar cross section reduction, reflective surface.

I. INTRODUCTION

IN recent years, there is an increasing interest in the design of a kind of artificial engineered surfaces that can be used to manipulate the backscattered Radar Cross Section (RCS) of objects [1]–[3]. Design of RCS reducer surfaces based on cross-polarization conversion principle have received a considerable attention recently [4]–[6]. Those surfaces are usually designed in such a way aiming to significantly reduce the backward scattered energy either by redirecting the reflected energy away from the direction it comes from or diffuse the incident EM waves into many different directions with low level lobes. The principle of coded metasurface was first introduced in [7]–[9] followed by several metasurfaces for RCS reduction such as [9]. In [8] a coding Metasurface was proposed around 10GHz to reduce the RCS of a solid PEC surface by carefully coding (“0” or “1”) the randomly distributed unit cells across the metasurface aperture.

In this article, a non-absorptive reflective surface for manipulating and reducing the backscattered RCS pattern of a solid PEC plate at W-band is presented. The presented reflective surface is designed based on cross-polarization conversion principle. The reflective surface is composed by simple Venus-like shape copper resonators which has three resonance plasmon frequencies at about 96GHz, 97.4GHz, and 99GHz with 100% polarization conversion efficiency at these frequencies. RCS reduction is achieved by randomly distributing the unit cell and it's mirrored one across the surface aperture to achieve the required reflection phase cancellation.

II. UNIT CELL DESIGN

As shown in Fig. 1, the unit cell consists of two copper layers separated by a high frequency dielectric substrate ($h=1.27\text{mm}$ and $\epsilon_r=10.2$). The upper layer consists of a Venus-like copper resonator and the lower layer is a solid copper ground plane. The cross- polarization conversion and reflection phase characteristics of the unit cell are investigated by performing a series of numerical simulations using F-solver of the full-wave CST microwave studio EM-package using unit cell boundary conditions in both $\pm x$ and $\pm y$ directions and a Floquet ports are assigned for calculations of co-polarization (co-pol) and cross-polarization (cross-pol) reflection coefficients along $\pm z$ directions. The final dimensions of the unit cell (and its mirrored unit cell) are optimized and the final values are presented in the caption of Fig.1.

The incident and reflected field components sketch are shown in Fig.1 (c) and (d) where pair of symmetric axes named u-axis and v-axis are introduced along $\pm 45^\circ$ directions with respect to y-axis. The calculated co-pol, cross-pol reflections and polarization conversion efficiency (PCR) coefficients versus frequency of the unit cell under normally incident plane wave are shown in Fig.2. Under normal incidence of EM-waves polarized along x- or y-axis, the cross-pol, co-pol and PCR terms used in this article are calculated using the formulas in Fig.2 (b), the subscripts i and r represents the incident and reflected waves, and the subscripts x and y denote the polarization direction of the incident EM waves, respectively. As can be seen in Fig.2 (a) strong cross-pol reflection (R_{xy} and R_{yx}) are occurred from about 95.7GHz to 99.3GHz for both x-polarized and y-polarized incident EM-waves. Furthermore, the unit cell has three plasmon resonance frequencies at about 96GHz, 97.4GHz, and 99GHz. Using the results of the co-pol and cross-pol reflection coefficients, the cross- polarization conversion efficiency (PCR) is calculated and the result is presented in Fig.2 (b) where the PCR is greater than 90% for the whole frequency band. As can be seen in Fig.1 (c) and (d) the incident EM-waves along x- or y-axis can be decomposed into two components along *u-axis* and *v-axis*. The reflection phase of the *u-axis* and *v-axis* reflected components versus frequency are calculated and the results are presented in Fig. 2 (c), the reflection phases from those two components are varies continuously from $+180^\circ$ to -180° because of the anisotropy of the proposed unit cell. The results in Fig.2 shows that the proposed unit cell can be used to compose a two-dimensional reflective surface that can efficiently rotates the incident

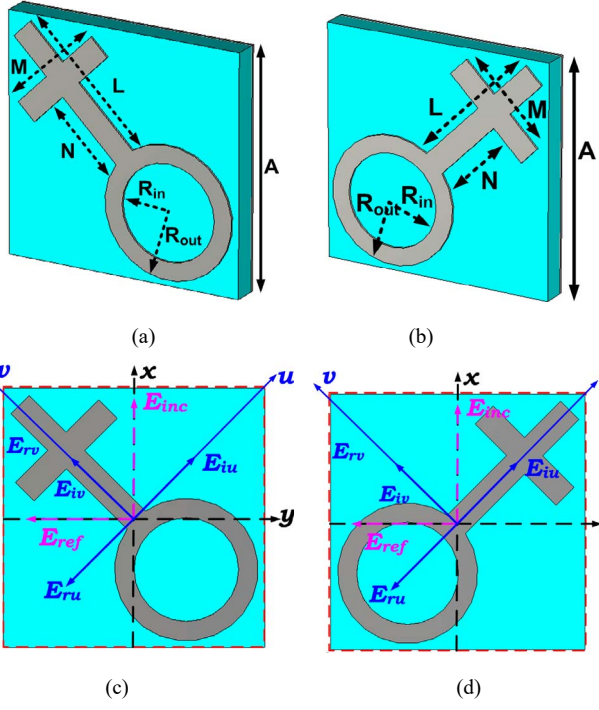


Fig. 1. Layout of the (a) proposed unit cell as “1” element: $L=0.7\text{mm}$, $S=0.4\text{mm}$, $A=2\text{mm}$, $g=0.3\text{mm}$, $W=0.2\text{mm}$, copper thickness=0.016mm, $\epsilon_r=10.2$ and $h=1.27\text{mm}$. (b) Mirrored unit cell as “0” element. (c) and (d) incident and reflected field components.

(x-polarized or y-polarized) EM waves into its cross-polarized (orthogonal) component. The possibility of using this unit cell for RCS reduction will be explained in the next section.

III. RCS REDUCTION INVESTIGATION

RCS reduction based on cross-polarization conversion Metasurface principle has been reported recently [4]-[6]. In 1-bit coded reflective surface, two unit cells with 180° reflection phase difference between their reflection phases are required. The results in Fig.2 (c) show that there is a clear reflection phase difference between the reflected waves from u -axis and v -axis as a result of the decomposition of the x- or y-axis linearly polarized incident EM waves and the computed phase difference is presented in Fig.3. As can be seen the reflection phase difference varies from about $180^\circ - 30^\circ$ to $180^\circ + 30^\circ$ over frequency band from 95.7GHz to 99.3GHz. To obtain the required phase difference between the adjacent cells across the RCS reducer reflective surface aperture, 1-bit coding can be done by using both the proposed unit cell as “0” element and its mirrored unit cell as “1” element with 0° and 180° phase responses, respectively, as shown in Fig.1 (a) and (b). The best unit cells distribution across the proposed surface aperture is optimized a special MATLAB code as shown in Fig.4. The 3D backscattered far-field RCS patterns of this surface and its equivalent bare PEC plate (for comparison purposes) are evaluated using the T-Solver of CST MWS and presented in Fig.4 (c), (d), (e) and (f) where the proposed reflective surface is placed in xy-plane. As can be seen when x-polarized or y-polarized EM plane wave normally incident on the proposed random reflective surface in Fig.4 (a), EM-waves will not be reflected according to Snell’s law of reflection as shown in Fig.4 (e) and (f) and the incident EM-wave is

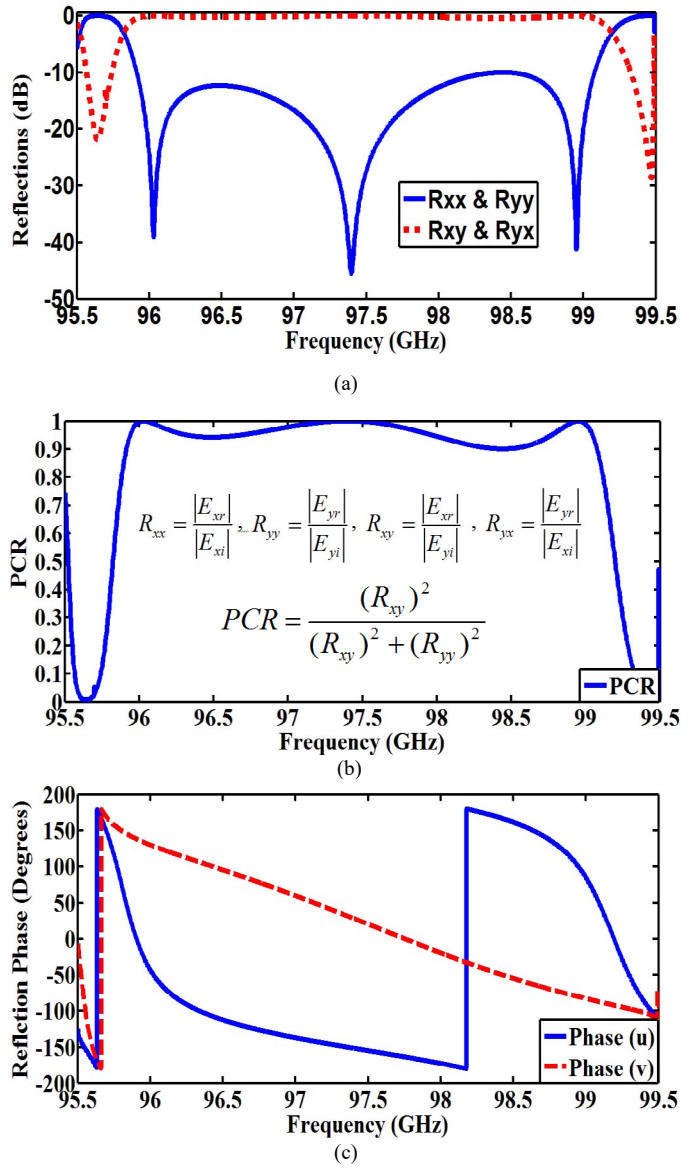


Fig. 2. Reflection characteristics of the proposed unit cell: (a) the co- and cross polarization reflections, (b) the polarization conversion ratio (PCR) and (c) the reflection phase of an incident wave polarized along u-axis and v-axis.

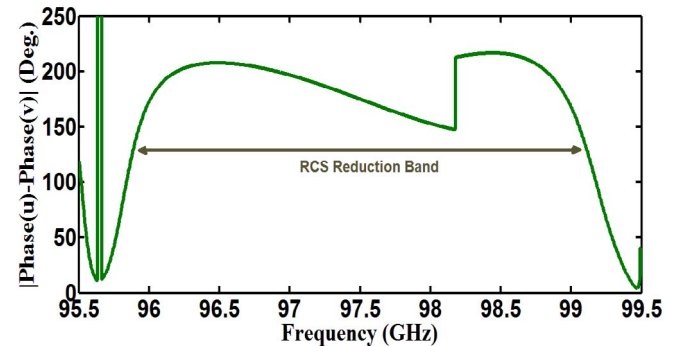


Fig. 3. Reflection phase difference between phases of the waves reflected from u-axis and v-axis.

reflected (diffused) in the half-space in front of the RCS reducer surface and distributed on a number of low level lobes in various directions because of the destructive interference and the RCS pattern would take a diffuse reflection pattern like shape. The 2D plot of the backscattered RCS pattern of a bare

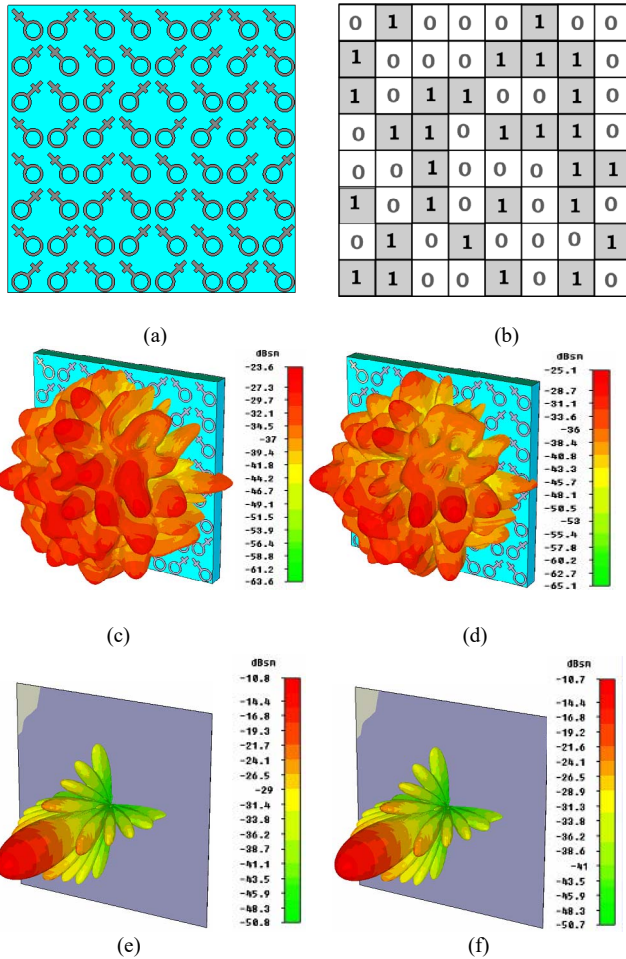


Fig. 4. (a) Layout of the random 1-bit RCS reducer surface, (b) unit cell distribution map, (c) and (d) are the 3D backscattered RCS patterns under normal incidence of the proposed surface at 95.6GHz and 95.8GHz, respectively, and their equivalent bare PEC plate in (e) and (f).

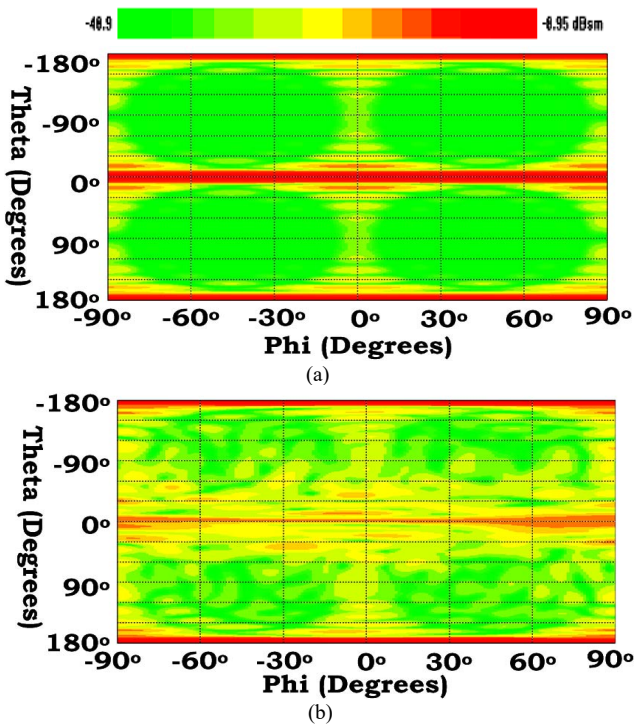


Fig. 5. 2D Plot of the backscattered RCS patterns of (a) bare PEC and (b) the proposed reflective surface.

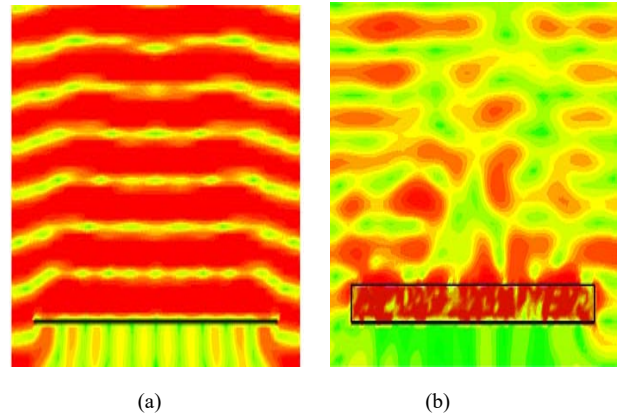


Fig. 6. the backscattered field distribution in front of the (a) PEC plate and (b) RCS reducer surface.

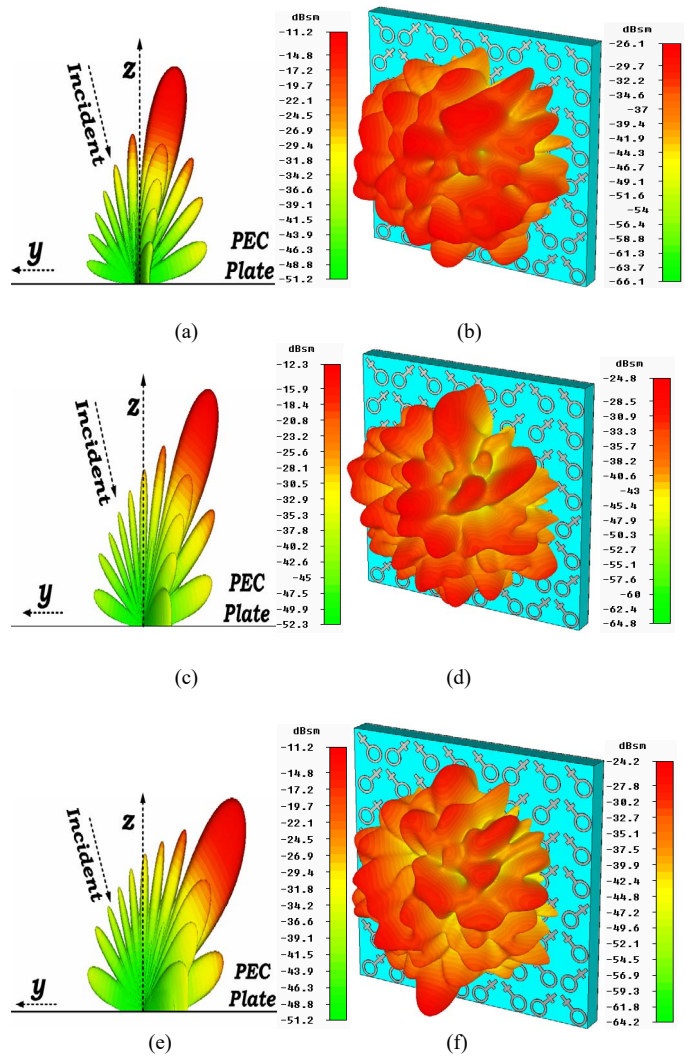


Fig. 7. Backscattered 3D RCS patterns under oblique incidence. (a) 15°, (c) 30° and (e) 45° for a bare PEC plate. (b) 15°, (d) 30° and (f) 45° for the proposed 1-bit reflective surface. All surfaces are placed in xy-plane.

PEC plate and the proposed 1-bit RCS reducer surface are presented in Fig.5 (a) and (b). As can be seen, for bare PEC surface the x-polarized or y-polarized normally incident EM-waves will be reflected as a single directive lobe ($\theta_i = \theta_r = 0^\circ$) as a result of the constructive interference, in other words

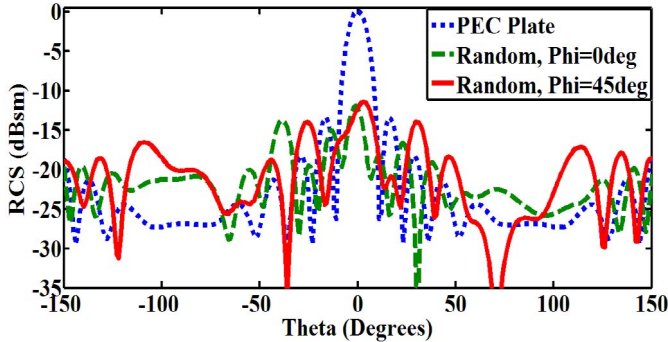


Fig. 8. Rectangular RCS far field pattern plot of the 1-bit surface.

specular reflection as. On the other hand, for the proposed surface with random distribution of unit cells according the distribution map in Fig.4 (b), the shape of the reflected RCS 2D pattern is changed to diffuse reflection with many low level lobes in various directions. The near field distribution of the backscattered energy in the half-space region in front of the surface and along the boresight direction is computed using T-solver of CST Microwave studio and the results are presented in Fig.6 (a) and (b) for both bare PEC and the proposed surface under normal incidence of EM waves. Near field distribution clearly shows that the normally incident EM-waves on the proposed surface is severely diffused and scattered back while for the bare PEC plate the incident EM-wave is reflected as a single directive beam along $\theta=0^\circ$ boresight direction as stated by Snell's law of reflection.

Furthermore, RCS reduction of the random surface under the incidence of y-polarized EM plane wave is investigated when the angle of incidence $\theta_{\text{inc}}=15^\circ$, 30° and 45° . Here θ_{inc} is the angle between z-axis and the direction of the incident plane wave. For the comparison purposes the RCS patterns of an equal size PEC plate is computed as well as shown in Fig.7 at 96GHz. As can be seen the proposed reflective surface still have a low level backscattered diffused pattern when the angle of incidence increase from zero degree to 15° , 30° , and 45° . On the other hand, the bare PEC plate reflects the incident waves as single directive lobe according to Snell's law of reflection (which states that the angle of incidence equals the angle of reflection). Figure 8 shows the rectangular plot of the backscattered RCS pattern in $\phi=0^\circ$ and $\phi=45^\circ$ planes (ϕ is the azimuth angle), as can be seen the backscattered diffuse reflection level is low in all directions compared to the classical bare PEC plate. All these results confirm that the proposed random surface can effectively manipulate the backscattered EM-wave.

IV. CONCLUSION

In this paper the design of RCS reducer surfaces based on cross-polarization conversion in mmWave regime is presented. The unit cell composing the surface has Venus-like metallic resonators and has three plasmon resonance frequencies at 96GHz, 97.4GHz, and 99GHz. The results shows that the presented surface can efficiently convert x- or y-polarized incident EM-waves to its orthogonal component with greater than 90% polarization conversion efficiency. Moreover, the proposed unit cell is used to design 1-bit coded RCS reducer

surface with optimized random unit cell distribution that can efficiently manipulate the backscattered RCS pattern shape.

ACKNOWLEDGMENTS

The authors would like to thank the National Natural Science Foundation of China for in part supporting of this work under Grant 61372077, in part by the Shenzhen Science and Technology Programs under Grant ZDSYS 201507031550105, JCYJ20170302150411789, JCYJ20170302142515949 and GCZX2017040715180580, as well as in part by the Guangdong Provincial Science and Technology Program under Grant 2016B090918080.

REFERENCES

- [1] D. Schurig, J. J. Mock, and B. J. Justice et.al. , "Metamaterial electromagnetic cloak at microwave frequencies" *Science*, vol.314, pp.977-980, 2006.
- [2] M. Paquay, J.C. Iriarte, and I. Ederra et.al., "Thin AMC Structure for Radar Cross-Section Reduction," *IEEE Trans. Antennas Propag.*, Vol.55, No.12, pp.3630-3638, 2007.
- [3] Tao Hong, Han Dong, and Jun Wang et.al., "A Novel Combinatorial Triangle-Type AMC Structure for RCS Reduction," *Microwave Optical Technol. Lett.*, Vol.57, No.12, pp.2728-2732, 2015.
- [4] H. Sun, et. al. , "Broadband and Broad-angle Polarization-independent Metasurface for Radar Cross Section Reduction," *Scientific Reports* 7, Article number: 40782, 2017.
- [5] W. Jiang, Y. Xue, and S. Gong, "Polarization Conversion Metasurface for Broadband Radar Cross Section Reduction," *Progress In Electromagnetics Research Letters*, vol. 62,pp. 9–15, 2016.
- [6] Y. Jia, Y. Liu, Y. J. Guo, K. Li and S. X. Gong, "Broadband Polarization Rotation Reflective Surfaces and Their Applications to RCS Reduction," *IEEE Transactions on Antennas and Propagation*, vol. 64, no. 1, pp. 179-188, 2016.
- [7] C. D. Giovampaola and N. Engheta, "Digital Metamaterials," *Nature Materials*, vol. 13, no. 12, pp.1115–1121, Dec 2014.
- [8] T. J. Cui, M. Q. Qi, X. Wan, J. Zhao, and Q. Cheng, "Coding Metamaterials, Digital Metamaterials and Programmable Metamaterials," *Light: Science and Applications*, 3, 2014.
- [9] L.-H. Gao, et al., "Broadband diffusion of terahertz waves by multi-bit coding metasurfaces," *Light: Science and Applications*, 4, 2015.